第32卷 第9期　焊 接 学 报　Vol. 32 No. 9
2011年9月　TRANSACTIONS OF THE CHINA WELDING INSTITUTION　September 2011

金属单质活性剂对镁合金 A-TIG 焊的影响

张兆栋， 曹全金
(辽宁省先进连接技术重点实验室 大连理工大学 材料科学与工程学院，大连 116024)

摘　要：以4种金属单质镉、锌、钛和铬作为镁合金 A-TIG 焊的活性剂，分析了不同金属单质对焊缝形貌、电弧形态及电弧电压的影响. 结果表明，与常规 TIG 焊相比，镉和锌活性剂均增加焊接熔深，钛活性剂对焊接熔深不起作用，铬活性剂反而减少焊接熔深；涂敷镉和锌时，焊接过程中电弧形态收缩，电弧电压增加；涂敷钛和铬对电弧形态和电弧电压基本没有影响. 镉和锌活性剂增加镁合金 A-TIG 焊接熔深的主要机理可能是受二者熔沸点和第一电离能的影响，使得在交流电正半波期间电弧导电通道收缩.

关键词：镁合金；活性剂；金属单质；A-TIG 焊
中图分类号：TG115.28　**文献标识码**：A　**文章编号**：0253-360X(2011)09-0037-04

张兆栋

0 序　言

镁合金具有比重轻、比强度高、减震性好和导热性优良等特点，被誉为21世纪最具潜能的工程结构材料，在汽车制造、航空航天、通讯、电子等行业备受青睐[1,2]. 镁合金作为一种新型的高性能材料，在实际应用中，不可避免地面临连接问题，而焊接无疑是一种优先的选择.

活性化焊接简称 A-TIG 焊，它最早是 Gurevich 与 Zamkov 在20世纪60年代提出的，但是直到20世纪90年代末期才在欧美国家的科研机构开展广泛的研究. 关于活性剂增加焊接熔深机理的研究，主要形成了两种理论，即电弧收缩理论[3]和表面张力温度梯度改变理论[4]. 目前，国内外对镁合金活性剂的研究主要集中在金属氯化物[5]和金属氧化物[6]上. 研究者通过试验分析认为氯化物增加熔深的机理主要是影响焊接电弧，而氧化物主要影响焊接熔池[7]. 但是，金属氧化物中的金属元素能否改变熔池金属流动方式，从而增加焊接熔深，研究者还未给出统一定论. 而且镁是一种活泼金属，其活动性位于铝之前，铝与金属氯化物在焊接过程中可发生置换反应[8]，因此镁也能够与金属氯化物发生置换反应生成金属氯化物中相应的金属，而这些金属能否影响焊接电弧，从而增加焊接熔深，国内外对此还研究很少.

试验通过选取4种物理性质各不相同的金属单质(镉、锌、钛、铬)作为镁合金活性剂，研究了这4种活性剂对焊缝形态、焊接电弧和电弧电压的影响，并结合活性剂的物理性质对金属单质增加焊接熔深的机理进行了初步探讨，旨在揭示金属单质对镁合金 A-TIG 焊接熔深的影响规律，为进一步解释金属氧化物或金属氯化物增加镁合金 A-TIG 焊接熔深的机理提供借鉴.

1 试验方法

试验采用尺寸为 100 mm × 100 mm × 6 mm 的 AZ31B 变形镁合金板材作为焊接试板，其化学成分见表1. 选用的4种金属单质活性剂为锌粉、镉粉、钛粉和铬粉. 焊接方法为直枪交流氩弧焊平板堆焊. 焊接前先对焊接试样进行打磨以去除表面氧化膜，再用丙酮去除表面油污. 为了使活性剂涂敷均匀，在使用活性剂之前先对活性剂粉末进行充分研磨，然后与丙酮均匀搅拌并混合成悬浊液，用毛刷使其均匀涂敷在试件表面.

表1　AZ31B 变形镁合金板材的化学成分(质量分数，%)
Table 1　Chemical compositions of AZ31B magnesium alloy

Al	Zn	Mn	Ca	Si	Cu	Mg
2.5~3.5	0.5~1.5	0.2~0.5	0.04	0.10	0.05	余量

为了便于与未涂敷活性剂时相比较，焊道只涂刷一半，焊接时涂敷区和未涂敷区一次焊接完成，如图1所示，左侧为未涂敷活性剂区域，右侧为涂敷活

收稿日期：2010-11-29
基金项目：国家自然科学基金资助项目(51004022)；辽宁省博士启动基金资助项目(20091010)

性剂区域. 试验中采用 CPL-MS25K 高速摄像机和氩光学干涉滤光片对焊接过程的氩电弧形态进行了正面观察，摄像机位置见图 1. 并采用泰克 TDS 1002 数字存储示波器采集电弧电压. 焊接过程中所需工艺参数如表 2 所示.

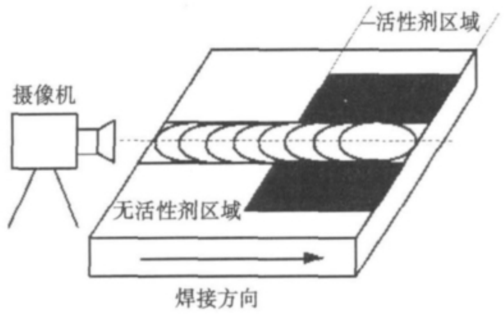

图 1 镁合金 AZ31B 试样 TIG/A-TIG 焊接示意图
Fig. 1 Schematic of AZ31B Mg alloy used in TIG/A-TIG welding

表 2 焊接工艺参数
Table 2 Welding parameters of A-TIG welding

焊接电流 I/A	焊接速度 v/(mm•min^{-1})	弧长 l/mm	保护气体流量 q/(L•min^{-1})	钨极直径 d/mm
120	300	1	15	3.2

2 试验结果

2.1 活性剂对焊缝表面及焊缝熔深的影响

图 2 为未涂敷活性剂和涂敷 4 种不同活性剂的焊缝表面成形. 从图 2b 中可以看出，加入镉粉的焊缝表面成形较好，无咬边、凹陷等焊接缺陷. 图 2c 所示的是加入锌粉的焊缝表面，从图 2c 中可以看出锌粉的加入使焊缝表面变得光滑、平整，但无明显的鱼鳞纹. 钛粉的加入没有改变焊缝表面形貌，基本上与未涂覆活性剂的一致，如图 2d 所示. 从图 2e 中可以看出，铬粉的加入使焊缝表面有所恶化，焊缝无鱼鳞纹且两侧存在大量熔渣.

从图 3 中可以看出，与常规 TIG 焊相比，涂敷锌粉后，焊接熔深增加效果最为明显; 其次是涂敷镉粉; 涂敷钛粉后，焊接熔深变化不大; 而涂敷铬粉后，焊接熔深变小.

图 4 所示的是未涂敷与涂敷 4 种不同活性剂的焊接熔深(h) 、熔宽(w) 和深宽比(h/w) 的对比. 从图 4 中可以看出，当使用锌粉时，焊接熔深、熔宽和深宽比均明显高于常规 TIG 焊，焊接熔深为常规 TIG 焊的 180%; 当使用镉粉时，焊接熔深、熔宽和深

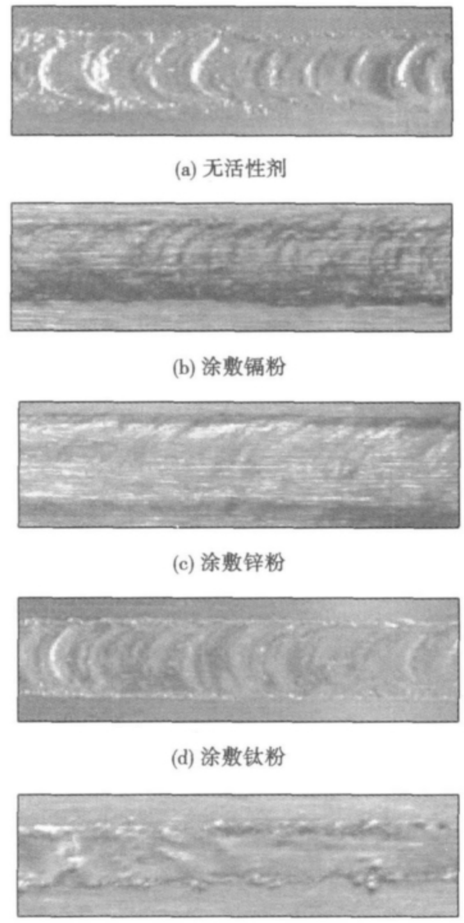

(a) 无活性剂
(b) 涂敷镉粉
(c) 涂敷锌粉
(d) 涂敷钛粉
(e) 涂敷铬粉

图 2 未涂敷和涂敷活性剂的焊缝表面成形
Fig. 2 Weld surface without and with fluxes

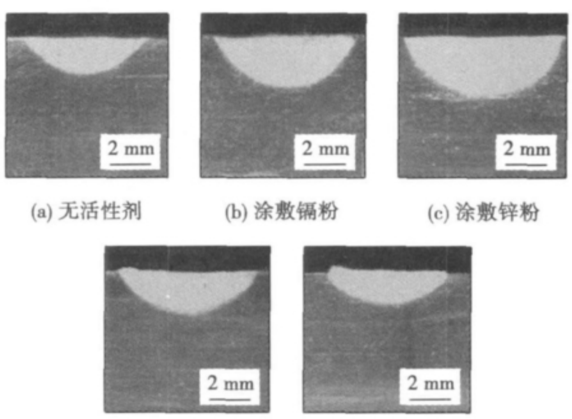

(a) 无活性剂 (b) 涂敷镉粉 (c) 涂敷锌粉
(d) 涂敷钛粉 (e) 涂敷铬粉

图 3 未涂敷和涂敷活性剂的焊缝横截面形貌
Fig. 3 Weld pool shapes without and with fluxes

宽比均高于常规 TIG 焊，焊接熔深为常规 TIG 焊的 150%; 当使用钛粉时，焊接熔深未发生明显变化，但焊接熔宽却大于常规 TIG 焊; 当使用铬粉时，焊接熔深、熔宽和深宽比均小于常规 TIG 焊，焊接熔深为常

规 TIG 焊的 90%.

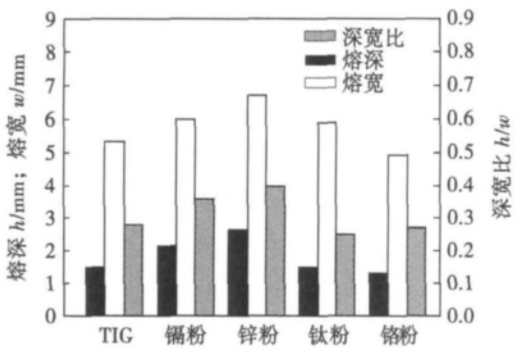

图 4　未涂覆和涂敷活性剂的焊接熔深、熔宽和深宽比

Fig. 4　Weld penetration, width and depth-to-width ratio without and with fluxes

2.2　活性剂对电弧形态的影响

镁合金常规 TIG 焊中，采用氩气作为保护气体，由于 Ar 元素本身的电离能较高，其只能在电弧中心温度较高的导电通道区域内发生电离，而电弧周围温度较低，氩很难被电离，所以氩电弧形态可以近似看成是电弧的导电通道. 试验采用高速摄像机和氩光学干涉滤光片对焊接过程的氩电弧形态进行了正面观察，以讨论电弧导电通道的变化情况，试验结果如图 5 所示.

为了保证电弧形态的准确性，图 5 所拍摄的氩电弧形态均是活性剂只涂刷一半，涂敷区和未涂敷区一次焊接完成(图 1) ，所得到的交流电正半波的电弧形态. 从图 5 中可以看出，涂敷镉粉和锌粉时，与未涂敷活性剂区域的氩电弧相比，电弧形态发生收缩，即导电通道发生收缩; 而涂敷钛粉和铬粉时，氩电弧形态并未发生明显变化.

2.3　活性剂对电弧电压的影响

表 3 所示的是与未涂敷活性剂区域相比，涂敷活性剂区域电弧电压的增加情况. 从表 3 中可以看出，锌粉加入后，电弧电压增加最大，为 2.3 ~ 3.2 V; 其次是镉粉，电弧电压增加 1.3 ~ 2.4 V. 而钛粉和铬粉的加入，基本上对电弧电压没有影响.

表 3　与未涂敷相比涂敷活性剂的电弧电压增加

Table 3　Increment of arc voltage with fluxes compared with that without flux

活性剂种类	与常规 TIG 焊相比电弧电压的增加 ΔU/V
镉粉活性剂	1.3 ~ 2.4
锌粉活性剂	2.3 ~ 3.2
钛粉活性剂	0.1
铬粉活性剂	0.1 ~ 0.2

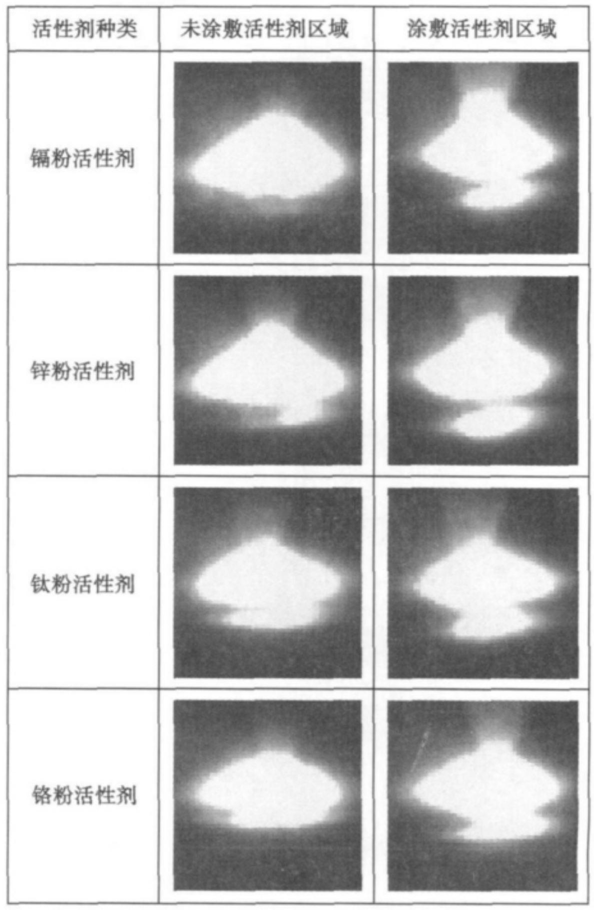

图 5　未涂敷和涂敷活性剂时交流电正半波的氩电弧形态

Fig. 5　Arc shape of Ar without and with fluxes during positive period of AC

3　分析与讨论

从试验结果来看，金属单质镉、锌可以增加镁合金 A-TIG 焊接熔深，而且二者的氩电弧形态比未涂敷活性剂的氩电弧形态有所收缩，电弧电压有较大增加. 但是单质钛对焊接熔深基本没有起作用，铬反而减少熔深，并且二者的电弧形态、电弧电压均与未涂敷活性剂的基本一致. 这说明活性剂的种类对镁合金 TIG 焊熔深增加作用影响很大，活性剂物理性质的差异将决定其作用机理.

3.1　熔沸点的影响

由于焊接时电弧本身的热量较高，而对于镁合金这样的低熔沸点材料，焊接过程中，不可避免的要发生熔化、蒸发现象. 对于镉单质和锌单质，其熔沸点均低于镁合金，如表 4 所示，而且镉单质和锌单质仅涂敷在镁合金板材表面，所以在焊接过程中，镉和锌更容易熔化、蒸发而进入电弧. 而对于钛单质和铬单质，由于二者的熔沸点较高(表 4) ，焊接过程又是在极短的时间内完成，所以钛和铬在焊接过程中很难蒸发而进入电弧.

表4 各种金属单质的熔沸点

Table 4 Melting point and boiling point of various metals

金属	熔点 T_m/K	沸点 T_b/K
Cd	593.9	1 038
Zn	692.7	1 180
Mg	922	1 363
Ti	1 933	3 560
Cr	2 130	2 945

3.2 第一电离能的影响

从图5的氩电弧形貌来看,镉和锌活性剂的加入,使得氩电弧形态比未涂敷活性剂时发生收缩. 这主要是因为镉和锌在电弧作用下,更容易熔化、蒸发而进入电弧,在电弧高温的作用下发生电离,而且二者的第一电离能均高于镁的第一电离能(表5),在电离相同数量电子的情况下,镉和锌用于电离而吸收的电弧热量要明显高于镁所吸收的热量,这就导致了电弧在维持正常放电的情况下,镉和锌的加入,使得电弧的热损失加大,根据最小电压原理,电弧具有保持最小能量消耗的特性. 因此,电弧会自动收缩其断面.

表5 各种元素的第一电离能(kJ/mol)

Table 5 First ionization energy of different elements

Ar	Zn	Cd	Mg	Ti	Cr
1 520.6	906.4	867.8	737.7	658.8	652.9

电弧收缩会使热量集中、电弧力集中,从而增加焊接熔深. 所以,镉和锌活性剂增加焊接熔深,主要是因为二者在正半波时,使氩电弧发生收缩,即电弧导电通道发生收缩,从而增加焊接熔深;同时,镉和锌活性剂使电弧导电通道收缩,势必造成电弧电压的升高,从表3中可得到证实. 而钛和铬由于本身熔沸点高,很难蒸发进入电弧,而且二者的第一电离能也低于镁(表5),因此其电弧形态和电弧电压不会产生类似镉和锌的效果,从图5和表3中可以得到证实,进而不可能增加焊接熔深. 而涂敷铬活性剂后,焊接熔深减小,这可能与涂敷铬活性剂焊缝表面的熔渣有关.

而对于镉和锌活性剂,二者的电弧收缩情况基本一致,但二者的电弧电压却发生了较大变化,这可能是因为锌的导热性要高于镉的导热性,使得涂敷锌活性剂的电弧传递给母材的热量要多于涂敷镉活性剂的,造成焊接过程中,涂敷锌活性剂的母材表面镁蒸发量要高于涂敷镉活性剂的镁蒸发量,从而增加了电弧弧长,使得涂敷锌活性剂的电弧电压高于涂敷镉活性剂的电弧电压.

4 结 论

(1) 锌单质和镉单质活性剂均可以增加镁合金交流A-TIG焊接熔深. 钛单质活性剂对焊接熔深不起作用,铬单质活性剂反而减少焊接熔深.

(2) 与常规TIG焊相比,涂敷镉和锌活性剂的氩电弧形态明显收缩,电弧电压有较大增加. 涂敷钛和铬活性剂对电弧形态和电弧电压基本没有影响.

(3) 金属单质镉和锌增加镁合金交流A-TIG焊接熔深的主要机理是:受二者熔沸点和第一电离能的影响,在交流电正半波期间电弧导电通道收缩,从而增加了焊接熔深.

参考文献:

[1] Mordike B L, Ebert T. Magnesium properties applications potential [J]. Material Science and Engineering, 2001, A302: 37-45.

[2] 宋 刚, 刘黎明, 王继锋, 等. 变形镁合金AZ31B的激光焊接工艺研究[J]. 应用激光, 2003, 23(6): 326-329.
Song Gang, Liu Liming, Wang Jifeng, *et al*. Study of YAG laser welding process on wrought magnesium [J]. Applied Laser, 2003, 23(6): 326-329.

[3] Howse D S, Lucas W. Investigation into arc constriction by active fluxes for tungsten inert gas welding [J]. Welding Research, 2002 (11): 291-298.

[4] Tanaka M, Shimizu T, Terasaki H, *et al*. Effects of activating flux on arc phenomena in gas tungsten arc welding [J]. Science and Technology of Welding and Joining, 2000, 5(6): 397-402.

[5] Marya M. Theoretical and experimental assessment of chloride effects in the A-TIG welding of magnesium [J]. Welding in the World, 2002, 46(8): 7-21.

[6] Liu Liming, Zhang Zhaodong, Song Gang, *et al*. Mechanism and microstructure of oxide fluxes for gas tungsten arc welding of magnesium alloy [J]. Metallurgical and Materials Transactions A, 2007, 38: 649-658.

[7] Zhang Zhaodong, Zhang Fan. Spectral analysis of welding plasma of magnesium alloy using flux coated wire [J]. Materials Transactions, 2009, 50(8): 1909-1914.

[8] 黄 勇, 樊 丁, 邵 锋. 铝合金活性TIG焊熔池表面化学反应分析[J]. 焊接学报, 2010, 31(5): 41-44.
Huang Yong, Fan Ding, Shao Feng. Analysis of chemical reaction on weld pool surface in activating TIG welding of aluminum alloys [J]. Transactions of the China Welding Institution, 2010, 31(5): 41-44.

作者简介: 张兆栋,男,1981年出生,博士,讲师. 研究方向为镁合金活性焊接技术. Email: skyezzd@dlut.edu.cn

Key words: 35CrMnSi steel; electron beam welding; microstructure; mechanical properties

Effects of metal activating fluxes on A-TIG welding of magnesium alloy ZHANG Zhaodong, CAO Quanjin (Key Laboratory of Liaoning Advanced Welding and Joining Technology, School of Materials Science and Engineering, Dalian University of Technology, Dalian 116024, China). p 37 – 40

Abstract: Four kinds of metal cadmium, znic, titanium and chromium were used as the activating fluxes for the A-TIG welding of magnesium alloy and the influence of metal activating fluxes on the weld morphology, the arc shape and the arc voltage has been analyzed. The results indicated that compared with the conventional TIG welding, both znic flux and cadmium flux increased the weld penetration depth, while the chromium flux redcued it and the effect of Ti flux was negligible. It could also be observed that the arc concentrated and the arc voltage increased with both znic and cadmium fluxes, while the variations of the arc and the arc voltage with titanium and chromium fluxes were hardly be observed. The main mechanism that znic and cadmium activating fluxes enhance weld penetration for the A-TIG welding of magnesium alloy may be that these fluxes constrict the current-conducting channel of the arc during the positive period of alternating current, due to the effect of the melting point, the boiling point and the first ionization energy.

Key words: magnesium alloy; activating flux; metal; A-TIG welding

Research on wear resistance of compound material surfacing alloy with high vanadium content ZONG Lin[1,2], LIU Zhengjun[2], GAO Hailiang[2], LI Lecheng[2] (1. School of Mechanical Engineering, Shenyang University of Chemical Technology, Shenyang 110142, China; 2. School of Material Science and Engineering, Shenyang University of Technology, Shenyang 110870, China). p 41 – 44, 48

Abstract: In order to study the wear resistant composite material with high Vanadium content, Fe-Cr-V-C alloy system was designed with plasma arc surfacing. The mechanical properties of surfacing overlays were examined with Rockwell hardometer and wear testing machine respectively. The phase composition, shape and distribution of microstructure have been researched by XRD, OM and SEM. The results showd that the mechanical properties of the surfacing overlay improved with the increasing of vanadium content. When the vanadium content was up to 26.2 percent, the mechanical properties of surfacing overlay obtained optimum value, the hardness was 64.9 HRC and the wear loss was 0.078 4 g. The numbers of vanadium carbide increased with the increasing of vanadium content. vanadium carbide particles diffused in the martensite matrix and formed wear resistant structure with $(Fe, Cr, V)_7C_3$ which distributed along grain boundaries. In a word, the property of wear resistance of surfacing overlay is very good.

Key words: surfacing alloy; plasma arc; surfacing; wear resistance

Feature extraction and image processing for underwater weld with laser vision LIU Suyi, LI Bing, ZHANG Hua, JIA Jianping (Robot and Weld Automation Key Lab., Nanchang University, Nanchang 330031, China). p 45 – 48

Abstract: Automation and intelligence are the development direction for underwater welding, and real-time sensing and detecting of underwater weld position is a key technology, among which laser vision sensing is a good-prospect detecting method. Noise features of weld image under different water environment and underwater V-groove weld image pre-processing are discussed. And both the application of mean shift algorithms on underwater weld image segmentation and linear Hough transform on extracting image features of underwater weld are studied. Experiment results show, after image enhancement and filtering, laser stripe including weld features could be effectively segmented with mean shift algorithms, and linear Hough transform was suited for precisely extracting V-groove weld feature points on the basis of thinning images.

Key words: feature extraction; image segmentation; underwater weld; laser vision

Ultrasonic testing technology of weld defect based on video positioning HU Wengang, GANG Tie, WANG Jinhai (State Key Laboratory of Advanced Welding Production Technology, Harbin Institute of Technology, Harbin 150001, China). p 49 – 52

Abstract: Manual ultrasonic testing system of weld defects based on video positioning of USB camera was studied. The planar position of ultrasonic probe relative to the weld bead was obtained by USB camera, and the depth of weld defects was obtained by ultrasonic probe. Then the locational qualitative and quantitative analysis on weld defects was obtained by the method of three-view projection imaging technology intuitively. This system is applicable to the field test of welded structure on service. Ultrasonic testing was performed to the actual weld, including crack defect by this system. The result showed that the location, size and distribution of weld defects could be characterized conveniently, quickly and intuitively, and the method was helpful for the qualitative recognition of different weld defects.

Key words: ultrasonic testing; weld defect; video positioning; projection imaging

Study on arc length control system for pulsed MIG welding of aluminum alloy LU Lihui[1], FAN Ding[2], HUANG Jiankang[1], ZHU Ming[1], SHI Yu[2] (1. Key Laboratory of Non-ferrous Metal Alloys and Processing, The Ministry of Education, Lanzhou University of Technology, Lanzhou 730050, China; 2. State Key Laboratory of Gansu Advanced Non-ferrous Metal Materials, Lanzhou University of Technology, Lanzhou 730050, China). p 53 – 56

Abstract: Research work of wire extension control based on vision sensing was done in pulsed MIG welding process of aluminum alloy. A rapid prototyping control platform was established for pulsed MIG welding of aluminum alloy using real-time target environment based on xPC. With vision sensing of welding zone image and corresponding image processing algorithm, a fuzzy PID closed loop control system for wire extension was designed on the basis of the built rapid prototyping control platform. Then experimental results showed that the method of vision sensing could meet the control requirements of wire extension stability, the rapid prototyping control system built with fuzzy PID controller based on vision sensing could realize the well control of the wire extension in pulsed MIG welding of aluminum alloy and also had strong robustness and quick response ability.

Key words: sliding mode controller; rapid prototyping;